Technical note: c-u-curve: A method to analyse, classify and compare dynamical systems by uncertainty and complexity

Uwe Ehret[1], Pankaj Dey[2]

[1]Institute of Water Resources and River Basin Management, Karlsruhe Institute of Technology (KIT), Karlsruhe, Germany
5 [2]Interdisciplinary Centre for Water Research, Indian Institute of Science, Bangalore, India

Correspondence to: Uwe Ehret (uwe.ehret@kit.edu)

Abstract. We propose and provide a proof-of-concept of a method to analyse, classify and compare dynamical systems of arbitrary dimension by the two key features uncertainty and complexity. It starts by subdividing the system's time-trajectory into a number of time slices. For all values in a time slice, the Shannon information entropy is calculated, measuring within-
10 slice variability. System *uncertainty* is then expressed by the mean entropy of all time slices. We define system *complexity* as "uncertainty about uncertainty", and express it by the entropy of the entropies of all time slices. Calculating and plotting uncertainty u and complexity c for many different numbers of time slices yields the *c-u-curve*. Systems can be analysed, compared and classified by the c-u-curve in terms of i) its overall shape, ii) mean and maximum uncertainty, iii) mean and maximum complexity, and iv) its characteristic time scale expressed by the width of the time slice for which maximum
15 complexity occurs. We demonstrate the method at the example of both synthetic and real-world time series (constant, random noise, Lorenz attractor, precipitation and streamflow) and show that the shape and properties of the respective c-u-curves clearly reflect the particular characteristics of each time series. For the hydrological time series we also show that the c-u-curve characteristics are in accordance with hydrological system understanding. We conclude that the c-u-curve method can be used to analyse, classify and compare dynamical systems. In particular, it can be used to classify hydrological systems
20 into similar groups, a precondition for regionalization, and it can be used as a diagnostic measure which can be used as an objective function in hydrological model calibration. Distinctive features of the method are i) that it is based on unit-free probabilities, thus permitting application to any kind of data, ii) that it is bounded, iii) that it naturally expands from single- to multivariate systems, and iv) that it is applicable to both deterministic and probabilistic value representations, permitting e.g. application to ensemble model predictions.

25

Keywords

Complexity, uncertainty, entropy, dynamical system analysis, catchment classification, catchment similarity.

1 Introduction

In the earth sciences, many systems of interest are dynamical, i.e. their states are ordered by time and evolve as a function of
30 time. The theory of dynamical systems (Forrester, 1968; Strogatz, 1994) therefore has proven useful across a wide range of earth science systems and problems such as weather prediction (Lorenz, 1969), ecology (Hastings et al., 1993; Bossel, 1986), hydrology (Koutsoyiannis, 2006), geomorphology (Phillips, 2006) and coupled human-ecological systems (Bossel, 2007).

Key characteristics of dynamical systems include their mean states (e.g. climatic mean values in the atmospheric sciences), their variability (e.g. annual minimum and maximum streamflow in hydrology) and their complexity (e.g. population
35 dynamics in ecological predator-prey cycles). Interestingly, despite its importance and widespread use there is to date no single agreed-upon definition and interpretation of complexity (Prokopenko et al., 2009; Gell-Mann, 1995), and many different concepts are employed across disciplines.

Characterizing dynamical systems by few and meaningful statistics representing the above-mentioned key features is important for several reasons: System classification, intercomparison and similarity analysis is a precondition for the transfer

40   of knowledge from well-known to poorly-known systems or situations (see e.g. Wagener et al., 2007; Sawicz et al., 2011; and Seibert et al., 2017 for applications in hydrology). Further, dynamical system analysis helps detecting and quantifying nonstationarity, a key aspect in the context of global change (Ehret et al., 2014), and it is important for evaluating the realism of dynamical system models and for guiding their targeted improvement (Moriasi et al., 2007; Yapo et al., 1998).

   In this paper, we address the task of parsimonious yet comprehensive characterization of dynamical systems by proposing a

45   method based on concepts of information theory. It comprises both variability and complexity, and adopts the view that the complexity of a time series is the overall variability of its variabilities in sub periods. We use examples from hydrology, as due to the multitude of subsystems and processes involved, most hydrological systems classify as complex systems (Dooge, 1986). Hydrological systems have been analysed and classified in terms of their complexity by Jenerette et al. (2012), Jovanovic et al. (2017), Ossola et al. (2015), Bras (2015), Engelhardt et al. (2009), Pande and Moayeri (2018), Sivakumar

50   and Singh (2012) and Sivakumar et al. (2007), among others. In the same context, concepts from information theory have been applied by Pachepsky et al. (2006), Hauhs and Lange (2008), Zhou et al., (2012), Castillo et al., (2015), and recently by Dey and Mujumdar (2021). Information-based approaches rely on log-transformed probability distributions of the quantities of interest, and are thus independent of the units of the data. Compared to methods relying directly on the data values, this poses an advantage in terms of generality and comparability across disciplines. Being rooted in information theory, the

55   method we propose in this paper makes use of this advantage. Compared to existing information-based methods, it offers the additional advantages of jointly considering two key characteristics of dynamical systems, uncertainty and complexity, and of being applicable to multivariate and ensemble data sets.

   The remainder of the text is organized as follows: In Sect. 2, we present all steps of the method. In Sect. 3, we apply the method to both synthetic time series and observed hydrological data. We use these examples to describe the properties,

60   interpretations and potential uses of the *c-u-curve* method. We summarize the method, discuss its limitations and draw conclusions in the final Sect. 4.

2 Method

   Please note that in what follows, for clarity we introduce the method at the example of univariate time series with deterministic values, and we also use the corresponding variable notation. In Ehret (2022) we also provide generalized

65   application examples for multivariate and ensemble cases, and the related generalized code. Also, we calculate discrete entropy based on a uniform binning approach. We do so as it has some useful properties (ease of interpretation is one of them) compared to calculating continuous entropy. Nevertheless, the method can also be used with non-uniform binning or continuous representations of data-distributions. For a detailed discussion of discrete vs. continuous entropy, see Azmi et al. (2021) and references therein.

70   **2.1 Method description**

   Applying the method to a given time series with overall nt time steps consists of a number of steps and related choices: At first, for each variate involved a suitable discretization (binning) scheme is chosen. The bins must cover the entire value range, and their total number nvb can be chosen according to a user's demands on data-resolution. Next, the time series is divided into a number of ns time slices. The slices must be mutually exclusive and together must cover the time series. The

75   slices are preferably, but not necessarily, of uniform width. Next, separately for each slice, a discrete probability distribution (histogram) is calculated using the data in the slice and the chosen binning scheme. From the so-obtained histogram, the Shannon information entropy H (Shannon, 1948) is calculated following Eq. (1),

$$H(X) = -\sum_{vb=1}^{nvb} p(x_{vb}) \cdot log_2(p(x_{vb}))$$

(1)

where $p(x_{vb})$ refers to the probability of variate value x falling into bin vb, and nvb is the total number of value bins. Entropy measures data variability or uncertainty in bit, with the intuitive interpretation as "the minimum number of binary

80 (Yes/No) questions needed to be asked to correctly guess values drawn from a known distribution". Cover and Thomas (2006) provide an excellent introduction to information theory, applications to hydrology and hydrometeorology are e.g. presented in Singh (2013) and Neuper and Ehret (2019). As entropy values may differ between slices, an overall uncertainty estimate for all slices is calculated as the expected value of all slice entropies. For equal-width slices, this is mean entropy according to Eq. (2),

$$Uncertainty = E\big(H(X)\big) = \overline{H(X)} = \frac{1}{ns} \cdot \sum_{s=1}^{ns} H_s(X) \tag{2}$$

85 where s refers to a particular slice of all ns time slices. The so-defined *uncertainty* measures average within-slice variability of the data, i.e. uncertainty of the time series as seen through the lens of the chosen time slicing scheme.

Next, we consider variability of entropy across all slices, and as before we measure variability by entropy. In order to calculate this higher-order "entropy of entropies", a suitable binning scheme for entropy values must be chosen, which can be based on the same criteria as outlined above. It is then used to calculate a histogram of the ns entropy values. We thus

90 define *complexity* as the entropy of entropy values, which is calculated following Eq. (3),

$$Complexity = H\big(H(X)\big) = -\sum_{eb=1}^{neb} p(H_{eb}) \cdot log_2(p(H_{eb})) \tag{3}$$

where neb denotes the total number of entropy bins, eb a particular entropy bin, and $p(H_{eb})$ the probability of a time slice entropy H_s falling into bin eb. Complexity measures how uncertain we are about the uncertainty in a particular time slice, when all we know is the distribution of uncertainties (entropies) across all time slices in the time series.

The entire procedure is repeated for many different choices of ns (time slicing schemes). For each choice of ns, for equal-

95 width slices the width of a time slice is $sw = nt/ns$. In principle, ns can be chosen to take any value in the range $[1,nt]$. For $ns = 1$, the entire time series is contained in a single slice of width $sw = nt$. For $ns = nt$, each time slice contains only a single time step. However, it is recommended to choose ns - and with it sw - from a smaller range: If we require that for a robust estimation of a time slice histogram, each of its nvb bins should on average be populated by a minimum number of m values, then the width sw of a time slice (i.e. the number of values within) must at least be $nvb \cdot m$ (see Eq. 4). This means

100 that for robust estimates of *uncertainty*, time slices should be wide. For robust estimates of *complexity*, however, it is the opposite: The histogram of uncertainty values is populated by a total of ns values (the entropies of all time slices). If we again require that each of the histogram bins should be populated by at least m values, then at least $neb \cdot m$ time slice entropy values are needed. This means that time slices should be narrow to accommodate many of them in a time series of a given length nt (see Eq. 2). Overall, for a user's choice of m, Eq. 4 yields the range of recommended time slice widths sw as

105 a function of time series length nt and the number of bins for both uncertainty (nvb) and complexity (neb).

$$\frac{nt}{neb \cdot m} \geq sw \geq nvb \cdot m \tag{4}$$

For example, for a time series with $nt = 30000$ time steps, and choices of $m = 3$, and $nvb = neb = 10$ (all histograms resolved by ten bins), the range of suitable time slice widths is [30,1000].

Throughout all time slicing schemes, the number of value and entropy bins must be kept constant to assure comparability. Together, the set of all time slicing schemes produces a set of complexity-uncertainty value pairs. Plotting them with

110 uncertainty values on the x-axis and complexity values on the y-axis is what we call the *complexity-uncertainty-curve*, or short *c-u-curve*. It summarizes several interesting properties of the time series under consideration, which will be discussed in Sect. 3.

3 Application to synthetic and real-world time series

3.1 Time series description

115   We discuss the properties of the c-u-curve at the example of six time series as shown in Fig. 1a-f. Time series a-c are synthetic time series: a straight line, random uniform noise, and the famous Lorenz attractor (Lorenz, 1963). We chose them for their simple, exemplary and well-known behaviour. The straight line (Fig 1a) contains no variability whatsoever and should therefore show both very little uncertainty and complexity. The random noise (Fig. 1b) contains very high, but constant variability and should therefore show high uncertainty and low complexity. The Lorenz attractor (Fig. 1c) is a prime

120   example of complex behaviour arising from feedbacks in dynamical systems. We used the code as provided by Moiseev (2022) with standard parameters to produce a time series of the Lorenz attractor. From its three variates, for clarity only the first one is shown and discussed, the results for jointly considering all three variates are similar. All synthetic time series consist of $nt = 30000$ time steps, and both for value binning and entropy binning ten bins were used. With a choice of $m = 3$, the range of recommended time slice widths is $sw = [30,1000]$ according to Eq. 4. In addition to the recommended range

125   of time slice widths, we also included the two extremes values $sw = 1$ and $sw = 30000$ for demonstration purposes.

Time series d-f are hydro-meteorological observations taken from the CAMELS US data set (Newman et al., 2015). The first (Fig. 1d) is daily precipitation observations for the South Toe River, NC (short: STR) basin, the second (Fig. 1e) is the corresponding time series of daily streamflow observations. The basin size is 113.1 km², and precipitation mainly falls as rain (fraction of precipitation as snow is 8.5%). The third time series (Fig. 1f) also contains daily streamflow observations,

130   but from the 111.5 km² Green River, MA (short: GR) basin, which is more snow-dominated (fraction of precipitation as snow is 22.2 %). We chose the time series for the following reasons: Comparing precipitation and streamflow series from the same basin (STR) allows analysing the effect of the rainfall-runoff transformation process on uncertainty and complexity. Here we expect that a basin - by spatio-temporal convolution of precipitation - mainly reduces precipitation variability, and with it uncertainty and complexity. Comparing streamflow from two basins with different levels of snow influence (STR and

135   GR) allows analysing the effect of snow processes on uncertainty and complexity. Here we expect that the carryover effect of snow accumulation, and the influence of an independent additional driver of hydrological dynamics – radiation – should increase both uncertainty and complexity. All hydro-meteorological time series contain 12418 daily observations from 1 October 1980 – 30 September 2014 (34 years). As for the synthetic time series, we also used ten bins to resolve both the range of values and the range of entropies. However, we used a different time slicing scheme to reflect standard ways of

140   time-aggregation of real-world data. In particular, we used the set of $sw = \{1,7,14,21,30,60,91,182,365,730,12418\}$ days, which corresponds to 1 day, 1-3 weeks, 1-6 months, 1-2 years, and the entire 34-year period. Please note that for a choice of $m = 3$, the range of recommended time slice widths is $sw = [30,414]$ days according to Eq. 4. Results for time slices outside of this range should therefore be treated with caution. We included them nevertheless for a more complete assessment of the time series.

145   We normalized all six time series to a [0,1] value range and then calculated uncertainty and complexity according to Eqs. (2) and (3). Normalizing the data is not a requirement, and it does not affect the shapes and values of the resulting c-u-curves. Rather it was a matter of convenience, as the same binning scheme could then be used for all time series.
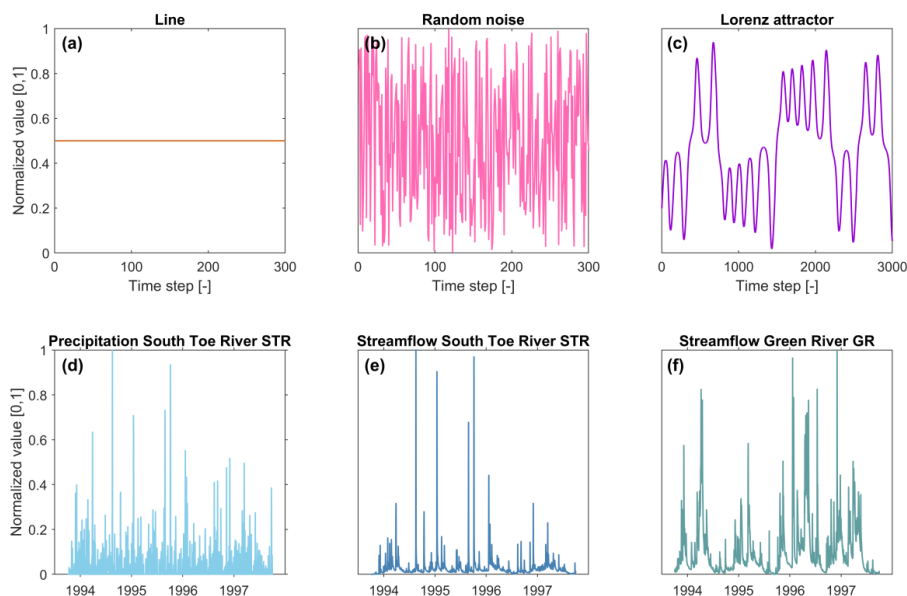
Figure 1. Synthetic and hydro-meteorological time series used for demonstration of the c-u-curve. Time series for subplots (a-c) comprise 30000 time steps; for clarity only 300 (subplots (a-b)) and 3000 (subplot c) time steps are shown. Time series for subplots (d-f) comprise 12418 daily time steps (34 years); for clarity only four years (1 October 1993 – 30 September 1997) are shown. All values are normalized to [0,1] value range. Further details on the time series are provided in the text.

3.2 Results and discussion

The c-u-curves of all six time series are shown in Fig. 2, and their key characteristics are summarized in Table 1. For clarity, Fig. 3 additionally shows only the hydro-meteorological time series in a sub region of Fig. 2. We start by discussing general properties of the c-u-curve, and then discuss properties of c-u-curves for each time series.

General properties. In Fig. 2 and Fig. 3, both axes are in bit, i.e. independent of the units of the data, thus facilitating intercomparison of different systems, and application to multivariate systems where variates are in different units. Further, for both uncertainty and complexity lower and upper bounds exist. Zero is the lower bound for both, indicating zero within-slice and across-slices variability. Upper bounds arise from the fact that for a given number of bins n, the maximum possible entropy is that of a uniform distribution, such that $H_{max} = H_{uniform} = log_2(n)$. For the ten bins chosen here, the upper limits are $log_2(10) = 3.3$ bit, shown as vertical and horizontal lines in Fig. 2, and horizontal line in Fig. 3. The values of the bounds, and all uncertainty and complexity values of the curve depend on the chosen binning. For direct comparison of c-u-curves, the binning should therefore agree. If this is for some reason not feasible, comparability can be established by normalizing values to a [0,1] range. This is possible due to the above-mentioned existence of upper and lower bounds and achieved by dividing values with their respective upper bound (not shown here). In addition to the existence of general upper and lower bounds, the values of uncertainty and complexity for extreme values of the time-slicing scheme are another general feature of the c-u-curve: For $ns = 1$, i.e. when the entire time series is contained in a single slice of width $sw = nt$, within-slice entropy is at its maximum and equals the entropy of the time series, and complexity is zero because only a single entropy value populates the entropy distribution. In Fig. 2 and Fig. 3, this limit is indicated by the right end of each c-u-curve. For $ns = nt$, each time slice is of width one and contains only a single time step. In such a case, within-slice entropy

is always zero, resulting in zero uncertainty and complexity, i.e. the c-u-curve will always start at the origin (see Fig.2 and Fig. 3).

175
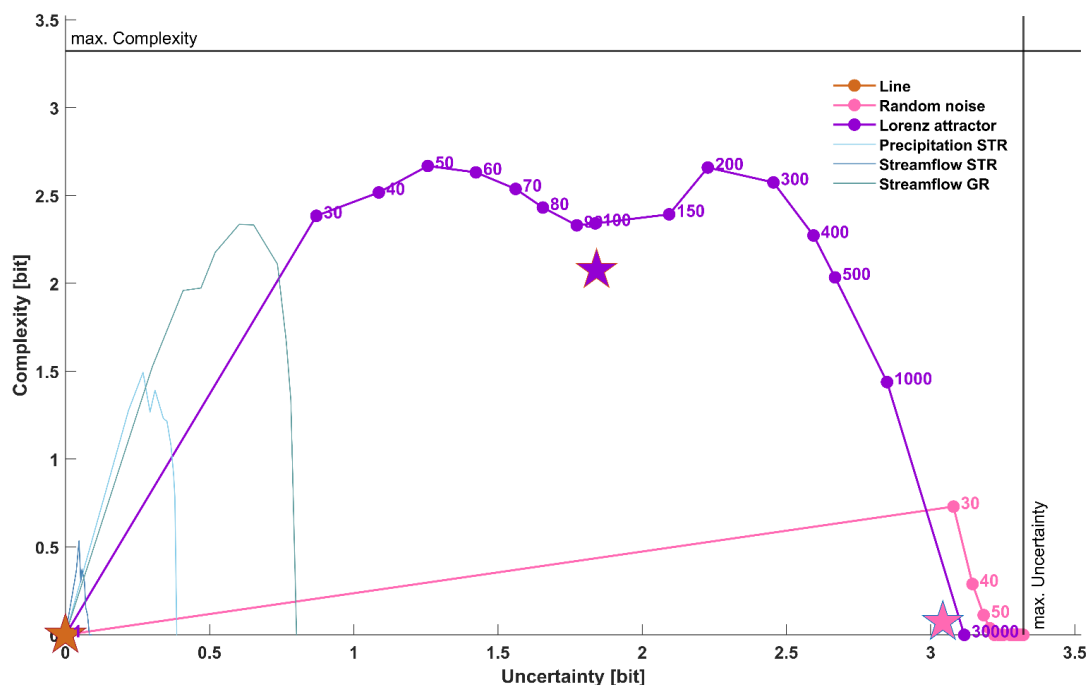
Figure 2. C-u-curves for synthetic (dotted) and hydro-meteorological (no marker) time series as shown in Fig. 1. Time series length is 30000 for the synthetic data and 12418 for the hydro-meteorological data. The number of value bins and entropy bins is ten, maximum uncertainty limit and maximum complexity limit is at $log_2(10) = 3.32$ bit. For the synthetic series, dot labels indicate the time slice width

180   sw used to calculate uncertainty and complexity, and the pentagram positions indicate mean uncertainty and mean complexity across all chosen time slicing schemes. The hydro-meteorological series are included to indicate their position within the full range of uncertainty and complexity; their details are shown in Fig. 3.

Apart from these general features, the overall shape of each c-u-curve contains key characteristics of the underlying time

185   series. We start by discussing the c-u-plot of the *straight line* in Fig. 2: It shows – as expected - the simplest behaviour: For all time-slicing schemes, both within-slice and across-slices variability is zero, i.e. the series displays zero uncertainty and complexity throughout (all dots are stacked at the origin). As a consequence, mean uncertainty and complexity across all time-slicing schemes (indicated by the brown pentagram in the plot and listed in Table 1) is also zero.

The *random noise* series in Fig. 2 on the contrary displays very high uncertainty and low complexity for most of the time

190   slicing schemes (most dots are stacked in the lower right corner of the plot), and only for many but narrow time slices of 50, 40 and 30 values per slice does complexity assume non-zero values. This can be attributed to random effects in small samples, where purely by chance both highly and hardly variable samples can occur, thus creating a wide range of time slice entropies, resulting in apparent non-zero complexity. For wider slices, the larger sample size leads to more similarly distributed samples, resulting in a narrow range of time slice entropies and hence low complexity. Overall, mean uncertainty

195   is very high and mean complexity is very low (position of the pink pentagram in Fig. 2 and values in Table 1), which is what we expected from random noise as a purely chaotic process.

The *Lorenz attractor* in Fig. 2 reveals a more diverse behaviour across the range of time slicing schemes. We start discussing it for the case of $sw = 30000$, i.e. when a single time slice covers the entire time series. As described in the general

200 properties, for this case uncertainty is always at its maximum and equals the entropy of the time series, and complexity is zero, because only a single entropy value populates the entropy distribution. The actual uncertainty value (3.11 bit), or its distance from the upper limit of uncertainty ($3.11/3.32 = 94\%$), is a key characteristic of the time series and expresses its overall variability. Decreasing the time slice width sw decreases within-slice variability (uncertainty). Also, it provides the potential for nonzero complexity as more and more entropy values populate the entropy distribution. For the curve shown in Fig. 2, complexity continuously increases and reaches its first maximum value of 2.66 bit (or $2.66/3.32 = 80\%$) for $sw =$

205 200 and at 2.22 bit of uncertainty. This point is another key characteristic of a c-u-curve, indicating at which temporal aggregation the across-slices variability is highest. Further decreasing slice width first leads to a decrease and then another increase in complexity until a second maximum of 2.66 bit is reached at $sw = 50$ (see values in Table 1). Afterwards, complexity and uncertainty decrease to zero for $sw = 1$, which is a general property of any c-u-curve (see discussion of general properties above). Taking the uncertainty and complexity mean across all time slices summarizes the c-u-curve in a

210 single point (purple pentagram in Fig. 2, values in Table 1). For the Lorenz attractor, it reveals medium average uncertainty, and high average complexity. This is in accordance with expectations, as the Lorenz attractor is known for exhibiting complex behaviour. Interestingly, apart from revealing its generally complex behaviour, the c-u-curve also reveals at which particular time slice width complexity of the Lorenz attractor is at a maximum. This can be interpreted as a "characteristic time scale" of the time series.

215

Table 1. Key characteristics of the c-u-curves for both the synthetic and the hydro-meteorological time series.

Time series	Uncertainty (bit)		Complexity (bit)		Characteristic time scale (days)[a]
	max	mean	max	mean	
Line	0	0	0	0	n.a.
Random noise	3.32	3.04	0.67	0.06	30
Lorenz attractor	3.11	1.84	2.66	2.07	50, 200
Precipitation STR	0.38	0.30	1.49	0.88	14
Streamflow STR	0.09	0.06	0.53	0.17	14
Streamflow GR	0.80	0.57	2.33	1.45	60

[a] width of time slice at which maximum complexity occurred.

Next, we discuss the c-u-curves of the hydro-meteorological time series. In Fig. 2, they are indicated by the lines without

220 markers. It is immediately obvious that they all possess low uncertainty, much lower than the theoretical maximum (indicated by the vertical "max. Uncertainty" limit) and the random noise, and also lower than the Lorenz attractor. This is in accordance with our expectations, and a consequence of the typically high temporal autocorrelation of hydro-meteorological time series, which clearly separates them from purely random time series. For a better view of detail, we re-plotted the hydro-meteorological time series in a sub region of the uncertainty limits in Fig. 3, which we will refer to in the following.

225 Despite the generally low uncertainties, the *precipitation STR* time series in Fig. 3 displays considerable average complexity (indicated by the pentagram position), which can be explained by the existence of meteorological regimes with different levels of precipitation variability, such as dry periods (low variability), periods with alternating dry and wet periods (high variability), and wet times with diverse precipitation amounts (high variability). The highest complexity occurs for a time slice width of $sw = 14$ days, indicating that the greatest variability of within-slice precipitation variability occurs for two-

230 week periods.

Interestingly, the corresponding *streamflow STR* time series displays much lower mean and maximum values (see Table 1) for both uncertainty (within-slice variability) and complexity (across-slices variability). This is in accordance with the general hydrological understanding that in the absence of major carryover mechanisms, rainfall-runoff transformation in

catchments is mainly by aggregation and convolution, thus reducing the variability of the precipitation signal. It is
235 noteworthy that while this harmonizing effect changes uncertainty and complexity means and maxima, it does not affect the
characteristic time scale: For streamflow STR - just as for precipitation STR - it is two weeks. This suggests that
precipitation remains the main control of streamflow complexity, despite the processes involved in rainfall-runoff-
transformation.

This is different for the second *streamflow GR* time series. Here, in addition to the above-mentioned rainfall-runoff
240 transformation, precipitation is partly stored as snow and later released as streamflow by melting. The temporal pattern of
snowmelt is not only governed by snow availability, i.e. the precipitation regime, but also energy availability, i.e. the long-
term radiation and temperature regime. Such additional, independent controls of hydrological function can add uncertainty
and complexity to streamflow production. Compared to streamflow STR, both uncertainty and complexity are indeed much
larger in terms of mean and maximum values, they are even larger than the corresponding values for precipitation STR
245 (compare pentagram positions in Fig. 3 and values in Table 1). The characteristic time scale of streamflow GR is at 2-3
months (60-91 days). This is considerably longer than for streamflow STR, and can be explained by the carryover effect of
snow accumulation and snowmelt acting at time scales in the order of months rather than days or weeks.
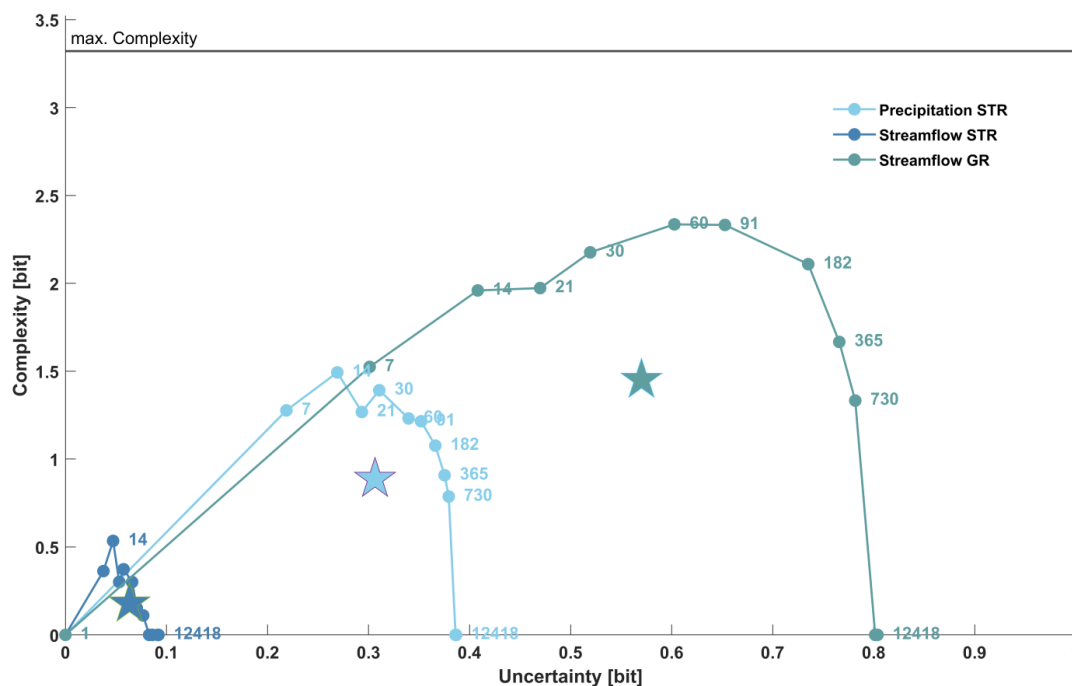
Figure 3. C-u-curves for all hydro-meteorological time series as shown in Fig. 1d-f. All time series comprise 12418 time steps, the number
250 of value bins and entropy bins is ten, maximum uncertainty limit and maximum complexity limit is at $log_2(10) = 3.32$ bit. Note that for
better display of details this is a horizontally zoomed-in version of Fig. 2. Dot labels indicate the time slice width *sw* used to calculate
uncertainty and complexity. The pentagram positions indicate mean uncertainty and mean complexity across all chosen time slicing
schemes.

4 Summary and conclusions

255

In this paper we presented a method to analyse and classify dynamical systems by the two key features uncertainty and
complexity. After dividing the time series into a set of time slices, the Shannon information entropy is calculated for the data

in each time slice. *Uncertainty* is then calculated as the mean entropy of all time slices, *complexity* as the entropy of all

260   entropy values. Complexity thus expresses "uncertainty about uncertainty" in the time series. Calculating and plotting uncertainty and complexity for many time slicing schemes yields the *c-u-curve,* with key characteristics mean and maximum uncertainty, mean and maximum complexity, and the characteristic time scale of the time series. The latter is defined as the time slice width at which maximum complexity occurs.

The c-u-curve method has several useful properties: Independence from the units of the data (both uncertainty and complexity are expressed in bit), existence of upper and lower bounds for both uncertainty and complexity as a function of

265   the chosen data resolution, and bounded behaviour when approaching upper and lower limits of time-slicing: For a single time-slice containing all data, uncertainty equals the time series entropy and complexity is zero, for time-slices containing single values both uncertainty and complexity are zero. The c-u-curve method is applicable to single- and multivariate data sets, and to deterministic and probabilistic value representations (ensemble data sets), making it suitable for a wide range of tasks and systems. The main limitation of the method arises from the requirement of sufficiently populating distributions,

270   which sets bounds to both the minimum and maximum width of time slices.

We provided a proof-of-concept at the example of six time series, three of them artificial, three of them from hydro-meteorological observations. The artificial time series (straight line, random noise, Lorenz attractor) were chosen for their very different, exemplary and well-known behaviour, and with the goal to demonstrate that the c-u-curve successfully reveals this behaviour, i.e. to demonstrate the general applicability of the method across a wide range of time series types.

275   The observed time series (precipitation and streamflow from a mainly rainfall-dominated basin, and streamflow from a basin where additionally snow processes influence the hydrological function) were chosen with the goal to demonstrate that the c-u-curve method reveals characteristics of real-world time series that are in accordance with general knowledge of hydrological system functioning. For all time series, we could show that the c-u-curve properties were distinctly different among the time series – which indicates that the method has discriminative capabilities useful for system classification -, and

280   that the properties are in accordance with expectations based on system understanding – which indicates that the method captures relevant time series properties and expresses them in terms of uncertainty and complexity -.

While the range of applications presented in this paper is small, and mainly intended as a proof-of-concept, the results encourage further studies. Particularly for hydro-meteorological applications, we suggest that the c-u-curve method can be used for data-based system classification, which is a precondition for the important hydrological task of regionalisation, i.e.

285   the transfer of knowledge from well-observed to poorly-observed places. In this context, the c-u-curve and its characteristic values can be used in a fashion similar to current uses of the flow-duration curves. This is supported by the clear differences of c-u-curve properties between the two investigated streamflow time series. We further suggest that the c-u-curve and its characteristic values can be used as a useful additional objective function in hydrological model training: While standard hydrological objective functions such as Nash-Sutcliffe efficiency guide models towards point-by-point agreement of models

290   output and observations, c-u-curve characteristics can guide models towards correct representations of short- and long-term variability patterns. Further work on this topic is in progress.

Code availability. The code used to conduct all analyses in this paper is publicly available at https://doi.org/10.5281/zenodo.5840045 (Ehret, 2022).

295

Data availability. All data used to conduct the analyses in this paper and the result files are publicly available at https://doi.org/10.5281/zenodo.5840045 (Ehret, 2022).

Author contributions. UE developed the c-u-curve method and wrote all related code. UE and PD designed the study

300   together and wrote the manuscript together.

Competing interests. The authors declare that they have no conflict of interest.

Acknowledgements. We gratefully acknowledge support by the Deutsche Forschungsgemeinschaft (DFG) and the Open
305 Access Publishing Fund of the Karlsruhe Institute of Technology (KIT). The second author acknowledges the funding
received from the research project "Advanced Hydrologic Research and Knowledge Dissemination" sponsored by the
Ministry of Earth Sciences (MoES), Government of India (Project No. MOES/PAMC/H&C/41/2013-PC-II).

Financial support. The article processing charges for this openaccess publication were covered by a Research Centre of the
310 Helmholtz Association.

References

Azmi, E., Ehret, U., Weijs, S. V., Ruddell, B. L., and Perdigão, R. A. P.: Technical note: "Bit by bit": a practical and general
approach for evaluating model computational complexity vs. model performance, Hydrol. Earth Syst. Sci., 25, 1103-
1115, 10.5194/hess-25-1103-2021, 2021.

315 Bossel, H.: Systems and Models. Complexity, Dynamics, Evolution, Sustainability, Books on Demand GmbH, Norderstedt,
Germany, 372 pp., 2007.

Bossel, H.: Dynamics of forest dieback: Systems analysis and simulation, Ecol. Model., 34, 259-288,
http://dx.doi.org/10.1016/0304-3800(86)90008-6, 1986.

Bras, R. L.: Complexity and organization in hydrology: A personal view, Water Resources Research, 51, 6532-6548,
320 10.1002/2015wr016958, 2015.

Castillo, A., Castelli, F., and Entekhabi, D.: An entropy-based measure of hydrologic complexity and its applications, Water
Resources Research, 51, 5145-5160, 10.1002/2014wr016035, 2015.

Cover, T., and Thomas, J. A.: Elements of Information Theory, Wiley Series in Telecommunications and Signal Processing,
Wiley-Interscience, 2006.

325 Dey, P., and Mujumdar, P.: On the statistical complexity of streamflow, Hydrological Sciences Journal, 1-14,
10.1080/02626667.2021.2000991, 2021.

Dooge, J. C. I.: Looking for hydrologic laws, Water Resour. Res., 22, 46S-58S, 10.1029/WR022i09Sp0046S, 1986.

Ehret, U.: KIT-HYD/c-u-curve: Version 1.0 (1.0.0). Zenodo. https://doi.org/10.5281/zenodo.5840045, 2022.

Ehret, U., Gupta, H. V., Sivapalan, M., Weijs, S. V., Schymanski, S. J., Blöschl, G., Gelfan, A. N., Harman, C., Kleidon, A.,
330 Bogaard, T. A., Wang, D., Wagener, T., Scherer, U., Zehe, E., Bierkens, M. F. P., Di Baldassarre, G., Parajka, J., van
Beek, L. P. H., van Griensven, A., Westhoff, M. C., and Winsemius, H. C.: Advancing catchment hydrology to deal with
predictions under change, Hydrol. Earth Syst. Sci., 18, 649-671, 10.5194/hess-18-649-2014, 2014.

Engelhardt, S., Matyssek, R., and Huwe, B.: Complexity and information propagation in hydrological time series of
mountain forest catchments, Eur. J. For. Res., 128, 621-631, 10.1007/s10342-009-0306-2, 2009.

335 Forrester, J. W.: Principles of Systems (2nd ed.), Productivity Press, Portland, OR, 391 pp., 1968.

Gell-Mann, M.: What is complexity? Remarks on simplicity and complexity by the Nobel Prize-winning author of The
Quark and the Jaguar, Complexity, 1, 16-19, 10.1002/cplx.6130010105, 1995.

Hastings, A., Hom, C. L., Ellner, S., Turchin, P., and Godfray, H. C. J.: Chaos in Ecology - Is Mother Nature a Strange
Attractor?, Annu. Rev. Ecol. Syst., 24, 1-33, 1993.

340 Hauhs, M., and Lange, H.: Classification of Runoff in Headwater Catchments: A Physical Problem?, Geography Compass,
2, 235-254, https://doi.org/10.1111/j.1749-8198.2007.00075.x, 2008.

Jenerette, G. D., Barron-Gafford, G. A., Guswa, A. J., McDonnell, J. J., and Villegas, J. C.: Organization of complexity in water limited ecohydrology, Ecohydrology, 5, 184-199, 10.1002/eco.217, 2012.

Jovanovic, T., Garcia, S., Gall, H., and Mejia, A.: Complexity as a streamflow metric of hydrologic alteration, Stochastic Environmental Research and Risk Assessment, 31, 2107-2119, 10.1007/s00477-016-1315-6, 2017.

Koutsoyiannis, D.: On the quest for chaotic attractors in hydrological processes, Hydrol. Sci. J.-J. Sci. Hydrol., 51, 1065-1091, 10.1623/hysj.51.6.1065, 2006.

Lorenz, E. N.: Predictability of a flow which possesses many scales of motion, Tellus, 21, 289-308, 1969.

Lorenz, E. N.: Deterministic Nonperiodic Flow, Journal of Atmospheric Sciences, 20, 130-141, 10.1175/1520-0469(1963)020<0130:Dnf>2.0.Co;2, 1963.

Moiseev, I.: Lorenz attractor plot (https://www.mathworks.com/matlabcentral/fileexchange/30066-lorenz-attaractor-plot), MATLAB Central File Exchange. Retrieved January 3, 2022.

Moriasi, D. N., Arnold, J. G., Van Liew, M. W., Bingner, R. L., Harmel, R. D., and Veith, T. L.: Model evaluation guidelines for systematic quantification of accuracy in watershed simulations, Transactions of the Asabe, 50, 885-900, 10.13031/2013.23153, 2007.

Neuper, M., and Ehret, U.: Quantitative precipitation estimation with weather radar using a data- and information-based approach, Hydrol. Earth Syst. Sci., 23, 3711-3733, 10.5194/hess-23-3711-2019, 2019.

Newman, A. J., Clark, M. P., Sampson, K., Wood, A., Hay, L. E., Bock, A., Viger, R. J., Blodgett, D., Brekke, L., Arnold, J. R., Hopson, T., and Duan, Q.: Development of a large-sample watershed-scale hydrometeorological data set for the contiguous USA: data set characteristics and assessment of regional variability in hydrologic model performance, Hydrol. Earth Syst. Sci., 19, 209-223, 10.5194/hess-19-209-2015, 2015.

Ossola, A., Hahs, A. K., and Livesley, S. J.: Habitat complexity influences fine scale hydrological processes and the incidence of stormwater runoff in managed urban ecosystems, J. Environ. Manage., 159, 1-10, 10.1016/j.jenvman.2015.05.002, 2015.

Pachepsky, Y., Guber, A., Jacques, D., Simunek, J., Van Genuchten, M. T., Nicholson, T., and Cady, R.: Information content and complexity of simulated soil water fluxes, Geoderma, 134, 253-266, https://doi.org/10.1016/j.geoderma.2006.03.003, 2006.

Pande, S., and Moayeri, M.: Hydrological Interpretation of a Statistical Measure of Basin Complexity, Water Resources Research, 54, 7403-7416, 10.1029/2018wr022675, 2018.

Phillips, J. D.: Deterministic chaos and historical geomorphology: A review and look forward, Geomorphology, 76, 109-121, 10.1016/j.geomorph.2005.10.004, 2006.

Prokopenko, M., Boschetti, F., and Ryan, A. J.: An information-theoretic primer on complexity, self-organization, and emergence, Complexity, 15, 11-28, https://doi.org/10.1002/cplx.20249, 2009.

Sawicz, K., Wagener, T., Sivapalan, M., Troch, P. A., and Carrillo, G.: Catchment classification: empirical analysis of hydrologic similarity based on catchment function in the eastern USA, Hydrol. Earth Syst. Sci., 15, 2895-2911, 10.5194/hess-15-2895-2011, 2011.

Seibert, S. P., Jackisch, C., Ehret, U., Pfister, L., and Zehe, E.: Unravelling abiotic and biotic controls on the seasonal water balance using data-driven dimensionless diagnostics, Hydrol. Earth Syst. Sci., 21, 2817-2841, 10.5194/hess-21-2817-2017, 2017.

Shannon, C. E.: A mathematical theory of communication, Bell system technical journal, 27, 623-656, citeulike-article-id:1584479, 1948.

Singh, V. P.: Entropy Theory and its Application in Environmental and Water Engineering, John Wiley & Sons, Ltd, 2013.

Sivakumar, B., and Singh, V. P.: Hydrologic system complexity and nonlinear dynamic concepts for a catchment classification framework, Hydrology and Earth System Sciences, 16, 4119-4131, 10.5194/hess-16-4119-2012, 2012.

385 Sivakumar, B., Jayawardena, A. W., and Li, W. K.: Hydrologic complexity and classification: a simple data reconstruction approach, Hydrol. Process., 21, 2713-2728, 10.1002/hyp.6362, 2007.

Strogatz, S. H.: Nonlinear Dynamics and Chaos: With applications to Physics, Biology, Chemistry and Engineering, Addison-Wesley Publishing Company, Reading, MA, 498 pp., 1994.

Wagener, T., Sivapalan, M., Troch, P., and Woods, R.: Catchment Classification and Hydrologic Similarity, Geography
390 Compass, 1, 901-931, https://doi.org/10.1111/j.1749-8198.2007.00039.x, 2007.

Yapo, P. O., Gupta, H. V., and Sorooshian, S.: Multi-objective global optimization for hydrologic models, Journal of Hydrology, 204, 83-97, 10.1016/s0022-1694(97)00107-8, 1998.

Zhou, Y., Zhang, Q., Li, K., and Chen, X. H.: Hydrological effects of water reservoirs on hydrological processes in the East River (China) basin: complexity evaluations based on the multi-scale entropy analysis, Hydrol. Process., 26, 3253-3262,
395 10.1002/hyp.8406, 2012.